


# Ca<sup>2+</sup>/calmodulin-dependent protein kinase II and protein kinase G oxidation contributes to impaired sarcomeric proteins in hypertrophy model

Kamilla Gömöri<sup>1,2,3†</sup>, Melissa Herwig<sup>2,4†</sup>, Heidi Budde<sup>2,4†</sup>, Roua Hassoun<sup>2,4</sup>, Nusratul Mostafi<sup>2,4</sup>, Saltanat Zhazykbayeva<sup>2,4</sup>, Marcel Sieme<sup>2,4</sup>, Suvasini Modi<sup>2,4</sup>, Tamara Szabados<sup>1,5</sup>, Judit Pipis<sup>1,5</sup>, Nikolett Farkas-Morvay<sup>1</sup>, István Leprán<sup>1</sup>, Gergely Ágoston<sup>6</sup>, István Baczkó<sup>1</sup>, Árpád Kovács<sup>2,4</sup>, Andreas Mügge<sup>4</sup>, Péter Ferdinandy<sup>3,5</sup>, Anikó Görbe<sup>1,3,5</sup>, Péter Bencsik<sup>1,5†</sup> and Nazha Hamdani<sup>2,3,4,7\*†</sup> 

<sup>1</sup>Department of Pharmacology and Pharmacotherapy, University of Szeged, Szeged, Hungary; <sup>2</sup>Institut für Forschung und Lehre (IFL), Molecular and Experimental Cardiology, Ruhr University Bochum, Bochum, Germany; <sup>3</sup>Department of Pharmacology and Pharmacotherapy, Semmelweis University, Budapest, Hungary; <sup>4</sup>Department of Cardiology, St. Josef-Hospital, Ruhr University Bochum, Bochum, Germany; <sup>5</sup>Pharmahungary Group Szeged, Hungary; <sup>6</sup>Institute of Family Medicine, University of Szeged, Szeged, Hungary; and <sup>7</sup>HCEMM-Cardiovascular Research Group, Department of Pharmacology and Pharmacotherapy, Semmelweis University, Budapest, Hungary

## Abstract

**Aims** Volume overload (VO) induced hypertrophy is one of the hallmarks to the development of heart diseases. Understanding the compensatory mechanisms involved in this process might help preventing the disease progression.

**Methods and results** Therefore, the present study used 2 months old Wistar rats, which underwent an aortocaval fistula to develop VO-induced hypertrophy. The animals were subdivided into four different groups, two sham operated animals served as age-matched controls and two groups with aortocaval fistula. Echocardiography was performed prior termination after 4- and 8-month. Functional and molecular changes of several sarcomeric proteins and their signalling pathways involved in the regulation and modulation of cardiomyocyte function were investigated.

**Results** The model was characterized with preserved ejection fraction in all groups and with elevated heart/body weight ratio, left/right ventricular and atrial weight at 4- and 8-month, which indicates VO-induced hypertrophy. In addition, 8-months groups showed increased left ventricular internal diameter during diastole, RV internal diameter, stroke volume and velocity-time index compared with their age-matched controls. These changes were accompanied by increased Ca<sup>2+</sup> sensitivity and titin-based cardiomyocyte stiffness in 8-month VO rats compared with other groups. The altered cardiomyocyte mechanics was associated with phosphorylation deficit of sarcomeric proteins cardiac troponin I, myosin binding protein C and titin, also accompanied with impaired signalling pathways involved in phosphorylation of these sarcomeric proteins in 8-month VO rats compared with age-matched control group. Impaired protein phosphorylation status and dysregulated signalling pathways were associated with significant alterations in the oxidative status of both kinases CaMKII and PKG explaining by this the elevated Ca<sup>2+</sup> sensitivity and titin-based cardiomyocyte stiffness and perhaps the development of hypertrophy.

**Conclusions** Our findings showed VO-induced cardiomyocyte dysfunction via deranged phosphorylation of myofilament proteins and signalling pathways due to increased oxidative state of CaMKII and PKG and this might contribute to the development of hypertrophy.

**Keywords** Volume-overload; Hypertrophy; Oxidative stress; Sarcomeric proteins

Received: 2 March 2022; Revised: 20 April 2022; Accepted: 4 May 2022

\*Correspondence to: Nazha Hamdani, Institut für Forschung und Lehre (IFL), Molecular and Experimental Cardiology, MABF 01/597, D-44780, Ruhr University Bochum, Bochum, Germany; Department of Cardiology, St. Josef-Hospital, Ruhr University Bochum, Bochum, Germany. Phone: +49-234-50959053; Fax: +49-234-3214904.  
Email: nazha.hamdani@rub.de

<sup>†</sup>These authors contributed equally to this work.

## Introduction

Mechanical load is one of the key drivers of cardiac remodelling as a result of the adaptation to the physiological or pathological stimuli.<sup>1</sup> Pathological mechanical load is categorized into pressure- and volume-overload. In response to volume overload (VO), eccentric hypertrophy occurs, in which chamber volume enlarges without a relative increase in its wall thickness. Cardiac hypertrophy is an adaptive consequence in response to various stressors,<sup>1,2</sup> however, excessive cardiac hypertrophic growth is maladaptive and results in cardiomyocyte dysfunction and thereby cardiac dysfunction. Mechanical stress is the trigger inducing a growth response in the overloaded myocardium. Various intracellular signals, responsible for the hypertrophic response via for example cytoskeleton proteins, may couple mechanical stress to modulation of gene expression, and/or protein synthesis to regulate/affect cardiomyocyte function.

Cardiac remodelling in human and experimental models of heart failure (HF) is characterized by impaired cardiomyocyte contraction and relaxation, as well as myocardial hypertrophy and accumulation of collagen in the extracellular matrix (ECM).<sup>3,4</sup> Cardiac stiffness is based on two main components: (i) the ECM, which provides the framework to interconnect the cardiomyocytes, containing fibrillar collagen and (ii) cardiomyocyte inner sarcomeric protein structure. VO induces changes in the abundance of protein such as proteins related to ECM, cytoskeleton, sarcomeres, cell-to-cell communication, and force transduction.

Cardiac muscle function is fine-tuned by phosphorylation and dephosphorylation of sarcomeric and calcium-handling proteins, including titin, cardiac myosin binding protein C (cMyBPC) and cardiac troponin I (cTnI).<sup>5</sup> Changes in myofilament proteins phosphorylation and alterations in cardiomyocyte mechanics are pathological features of the maladaptive remodelling in response to VO.<sup>6</sup> Phosphorylation is one of the major mechanisms by which the Ca<sup>2+</sup>-sensitivity of force development is regulated and contributes to fine tuning of the muscle function. Both cTnI and cMyBPC contain several phosphosites that are targeted by protein kinase A (PKA), protein kinase C (PKC), protein kinase G (PKG) or Ca<sup>2+</sup>-dependent calmodulin kinase II (CaMKII).<sup>7–11</sup> All these kinases are crucial for cardiomyocyte mechanical function.<sup>12,13</sup>

PKA-dependent phosphorylation of cTnI at Ser<sub>23/24</sub> is known to desensitize the myofilament to calcium,<sup>14</sup> additional to desensitization of myosin via cMyBPC phosphorylation by PKG and PKC. While CaMKII-dependent phosphorylation of cMyBPC was found to facilitate the phosphorylation of the two PKA phosphosites on cMyBPC.<sup>7,15</sup> Therefore, and given the fact that these proteins harbour multiple phosphorylation sites, the overall effect of the phosphorylation on myofilament function is defined by the crosstalk between different kinases/phosphatases.<sup>9,14</sup>

For the failing human heart significant alterations in the activities/expression levels of CaMKII have been reported, besides changes in PKA and PKC mediated phosphorylations.<sup>16–18</sup>

Previous research by us and others has demonstrated the role of oxidative stress and inflammation in altering various signalling pathways crucial for cardiomyocyte function among which are the kinases pathways.<sup>4,19</sup> Reactive oxygen species (ROS) might directly oxidize kinases or their targets leading to changes in their activity/binding affinity, respectively.<sup>19</sup> For example, oxidation of the regulatory CaMKII domain at Met<sub>281/282</sub> induces a Ca<sup>2+</sup>/CaM-independent activation.<sup>20,21</sup>

Through the regulation of Ca<sup>2+</sup> homeostasis and sarco/endoplasmic reticulum Ca<sup>2+</sup>-ATPase (SERCA) function, CaMKII $\delta$  is involved in cardiac remodelling and hypertrophic responses to mechanical overload.<sup>1,6</sup> While the impaired CaMKII $\delta$  signalling in mice models of pressure overload has been reported several times, not much is known about its contribution to VO induced hypertrophy.<sup>1,6</sup> In addition to its role in Ca<sup>2+</sup>-dependent signalling, CaMKII $\delta$  contributes to the regulation of cardiomyocyte stiffness mainly via titin phosphorylation.<sup>12,22</sup> Titin-based myocardial stiffness is regulated by posttranslational modifications including oxidation and phosphorylation. Titin spring elements, N2Bus and PEVK region, are targeted by multiple kinases leading to a distinct modulation of titin-based stiffness depending on the titin region and the kinase.<sup>12</sup> Titin is also a substrate for PKG and PKG1 $\alpha$  is the main isoform expressed in cardiac muscles, which is involved in phosphorylation of several cardiac target proteins and playing a crucial role in the sarcomere, Ca<sup>2+</sup> handling and hypertrophic gene expression.<sup>23</sup> PKG-dependent phosphorylation of N2Bus reduces titin stiffness thereby modulating diastolic function and relaxation and was shown to counter pathological remodelling and hypertrophy.<sup>24</sup> Oxidative stress-mediated attenuation of PKG pathway has been reported in HF with preserved ejection fraction (HFpEF), contributing to hypophosphorylation of titin via dysregulation of signalling pathways and a subsequent elevation in cardiomyocyte stiffness.<sup>25,26</sup>

The aim of the current study was to investigate the mechanisms of cardiomyocyte dysfunction in cardiac VO-induced hypertrophy through evaluating sarcomeric proteins and signalling pathways alteration that are responsible for cardiac contractility and relaxation. We investigated cTnI, cMyBPC, and titin, with a special focus on their PKG and CaMKII-dependent phosphorylation, and their contribution to the development of cardiac hypertrophic remodelling.

## Methods

### Animals

The present study conforms to the EU directive about the care and use of laboratory animals, published by the

European Union (2010/63/EU) and it was approved by the National Scientific Ethical Committee on Animal Experimentation and by the Ethics Committee for Animal Research of the University of Szeged (approval ID: XXVIII./171/2018.; on 24 January 2018).

Animals were housed in individually ventilated cages (Sealsafe IVC system, Tecniplast S.p.a., Varese, Italy), which conform the size recommendations of the abovementioned EU guidelines. Litter material (Lignocell hygienic animal bedding) placed beneath the cage and was changed at least three times a week. The animal room was temperature controlled ( $22 \pm 2^\circ\text{C}$ ) and had a 12-h light/dark cycle. Rats were fed with standard rodent chow and filtered tap water was available *ad libitum*.

### Volume overload-induced heart failure by aortocaval fistula

Two months old, male Wistar rats were anaesthetised by intraperitoneal (ip.) injection of pentobarbital sodium (Repose 50%, Le Vet. Pharma, Oudewater, Netherlands). Stomach area was shaved and disinfected with iodine solution (Braunol; B/Braun, B. Braun Medical, Sempach, Switzerland). After a midline laparotomy, the abdominal aorta was temporarily clipped between the left renal artery and the aortic bifurcation and the abdominal aorta was poked through with a G18 needle into the wall of the inferior vena cava, resulting in the formation of an aortocaval fistula, a short-cut for the bloodstream. Upon removal of the needle, tissue glue (cyanoacrylate glue, Loctite, Dusseldorf, Germany) was added on the surface of the aorta to seal the surface and to prevent bleeding. After surgery the animals were closed, provided proper wound care, and were administered with buprenorphine (0.05 mg/kg; ip.). Every effort was made to minimize the discomfort of the animals used in this study. Sham operated animals were used for controls underwent sham surgery, the same procedure as the treated groups except creation of the aortocaval fistula. For the development of volume overload-induced hypertrophy, animals were kept for 4 or 8 months, respectively ( $n = 5\text{--}6$  each group) (Figure 1A).

### Transthoracic echocardiography

At the end of 4 and 8 months, transthoracic echocardiography was carried out using a commercially available ultrasound machine (Vivid S5, GE Medical Systems, Budapest, Hungary) equipped with a 10.5 MHz 10S phased array cardiac sector probe. The left ventricular diameter, and ejection fraction were measured from parasternal long-axis view using M-mode images. The left ventricular stroke volume was assessed from the diameter of the left ventricular outflow

tract (LVOT), and time velocity integral of the LVOT was measured by pulsatile Doppler.

### Termination of animals

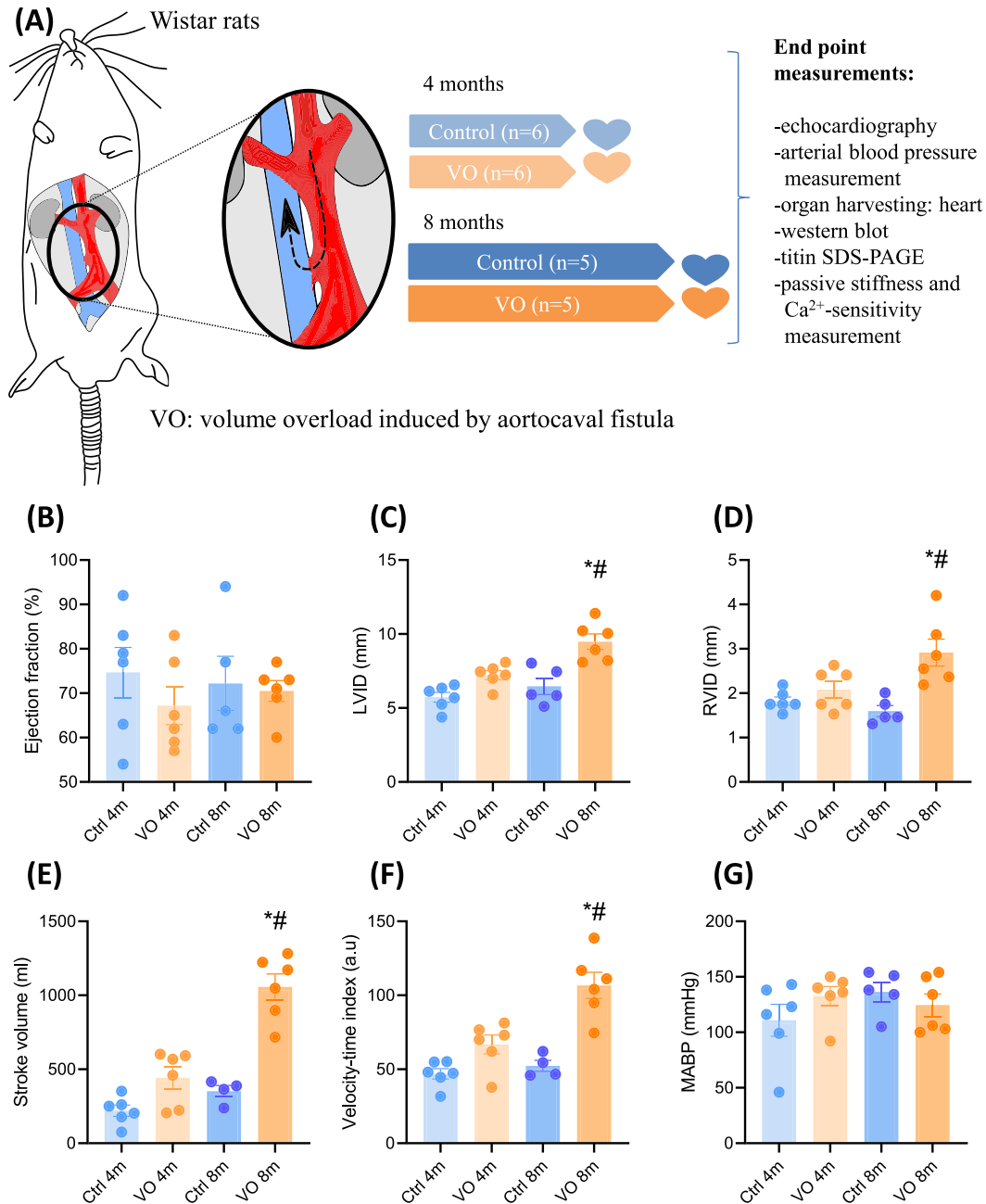
Male Wistar rats were anaesthetised by ip. injection of pentobarbital sodium (Repose 50%, Le Vet. Pharma, Oudewater, the Netherlands). Blood pressure, surface-lead electrocardiogram (ECG) were monitored for 10 min prior termination (Haemosys data acquisition system, Experimetria, Budapest, Hungary). The right carotid artery was cannulated for measurement of blood pressure. After collecting functional parameters of the heart, the animals were sacrificed and blood, heart and lung were harvested. Hearts were separated into left ventricle (LV), right ventricle (RV) and atria. Tissue was snap frozen in liquid nitrogen and kept in  $-80^\circ\text{C}$  freezer upon measurement.

### Western blot analyses

Left ventricular samples were solubilized in a modified Laemmli buffer (50 mM Tris-HCl at pH 6.8, 8 M urea, 2 M thiourea, 3% SDS w/v, 0.03% ServaBlue w/v, 10% v/v glycerol, 75 mM DTT, all from Sigma-Aldrich, St. Louis, MO, USA), heated for 3 min at  $96^\circ\text{C}$  and centrifuged for 3 min at  $4^\circ\text{C}$  and 14 000 rpm. From LV supernatant, 30  $\mu\text{g}$  of total protein/lane was loaded and separated by electrophoresis, 12% or 15% SDS gels were run at 90 V for 20 min following by 125 V for 90 min. Following SDS-PAGE, proteins were blotted onto polyvinylidene difluoride (PVDF) membranes (Immobilon-P 0.45  $\mu\text{m}$ ; Merck Millipore, Burlington, MA, USA). Blots were blocked with 5% bovine serum albumin (BSA) in Tween Tris-buffered saline (TTBS) for 1 h at room temperature (RT) and incubated with primary antibodies overnight at  $4^\circ\text{C}$  (Table 1). We used GAPDH (Sigma, 1:10000) for comparison of protein load.

After washing with TTBS, primary antibodies were detected with secondary horseradish peroxidase-labelled goat anti-rabbit antibody (DakoCytomation; catalogue number P0448 1:10 000) and enhanced chemiluminescence (Clarity Western ECL Substrate, BioRad). Imaging was carried out with ChemiDoc Imaging system (BioRad), bands were quantified by densitometry using the Image Lab software (version 6.1., Bio-Rad, Hercules, CA, USA) and Multi Gauge V3.2 software. Finally, signals obtained from the amount and phosphorylation were normalized to signals obtained from GAPDH stains referring to the entire protein amount transferred. Phosphoproteins are shown in ratio with their total protein. The obtained density values are expressed in arbitrary units (a.u.).

**Figure 1** Echocardiographic data. (A) Experimental set up, (B) ejection fraction, (C) LVID: left ventricle internal diameter in/during diastole, (D) RVID: right ventricle internal diameter, (E) stroke volume, (F) velocity-time index, (G) MABP: mean arterial blood pressure. Data are shown as mean  $\pm$  SEM;  $n = 5-6$ . \* $P < 0.05$ . 4-month versus 8-month and # $P < 0.05$  Ctrl versus VO using One way ANOVA Tukey multiple comparisons test.



### Titin expression and phosphorylation

To detect titin phosphorylation, LV samples were solubilized in a modified Laemmli buffer (50 mM Tris-HCl at pH 6.8, 8 M urea, 2 M thiourea, 3% SDS w/v, 0.03% ServaBlue w/v, 10% v/v glycerol, 75 mM DTT). For detecting titin oxidation,

*N*-ethylmaleimide instead of DTT was used for solubilization. Samples were heated at 96°C for 3 min, centrifuged for 3 min at 4°C at 14000 rpm, and then separated by agarose-strengthened 2% SDS-PAGE.<sup>27,28</sup> Gels were run at 2–4 mA constant current per gel for 16 h. Thereafter, western blot was performed to measure site-specific and total phosphory-

**Table 1** List of antibodies used for western blots

Antibody	Catalogue number	Company	Dilution
Total cardiac myosin binding protein C antibody	PA571701	Invitrogen	1:2000
Total cardiac troponin I antibody	ab 47003	Abcam	1:1000
Phospho-cardiac troponin I (Ser <sub>23/24</sub> ) antibody	40045	Cell Signaling Technology	1:1000
Phospho-cardiac troponin I (phospho Ser <sub>43</sub> ) antibody/mouse canonical sequence	ab 196005	Abcam	1:1000
Phospho-cardiac troponin I (phospho Thr <sub>143</sub> ) antibody	ab 58546	Abcam	1:1000
PKA C- $\alpha$ antibody	4782	Cell Signaling	1:1000
PKC $\alpha$ antibody	2056	Cell Signaling	1:1000
PKG antibody	13511	Cell Signaling	1:1000
CaMKII delta antibody	PA5-22168	Thermo Fisher Scientific	1:1000
CaMKII-phospho (Thr <sub>286</sub> ) antibody	12716	Cell Signaling Technology	1:1000
MAPK (ERK 1/2)	4695	Cell Signaling	1:1000
Phospho-MAPK (ERK 1/2)	4370S	Cell Signaling	1:1000
GAPDH	G9545	Sigma	1:10 000

lation of titin. Following SDS-PAGE, proteins were blotted onto polyvinylidene difluoride (PVDF) membranes (Immobilon-P 0.45  $\mu$ m; Merck Millipore, Burlington, MA, USA). Blots were preincubated with 3% bovine serum albumin in Tween Tris-buffered saline (TTBS; containing: 10 mM Tris-HCl; pH 7.6; 75 mM NaCl; 0.1% Tween; all from Sigma-Aldrich) for 1 h at RT followed by primary antibody incubation overnight at 4°C. For total titin phosphorylation anti-phospho-serine/threonine antibody (ECM Biosciences LLC; PP2551; 1:500) was used. For specific titin phospho-sites (phospho-Ser<sub>3991</sub>, -Ser<sub>4043</sub>, -Ser<sub>4080</sub>, -Ser<sub>12742</sub>, and -Ser<sub>12884</sub>) custom-made (by Eurogentec) antibodies were used.

The following custom-made rabbit polyclonal affinity purified antibodies were used:

- anti-phospho-N2Bus (Ser<sub>3991</sub>) against EEGKS (PO3H2) LSFPLA (dilution 1:500);
- anti-phospho-N2Bus (Ser<sub>4043</sub>) against QELLS (PO3H2) KETLFP (dilution 1:100);
- anti-phospho-N2Bus (Ser<sub>4080</sub>) against LFS (PO3H2)EWLRNI (dilution 1:500);
- anti-phospho-PEVK (Ser<sub>12742</sub>) against EVVLKS (PO3H2)VLRK (dilution 1:100);
- anti-phospho-PEVK (Ser<sub>12884</sub>) against KLRPGS (PO3H2) GGEKPP (dilution 1:500).

For titin oxidation, anti-GSH antibody (ab19534, Abcam, 1:500) was used. Both titin phosphorylation and oxidation were investigated by HRP-conjugated secondary anti-rabbit or anti-mouse antibodies (1:10 000), which were used next day for 1 h at RT, then blots were treated with ECL (Clarity Western ECL Substrate, BioRad) for developing chemiluminescence signal (see above). Chemiluminescence signals were normalized to signals obtained from Coomassie-stained PVDF membranes referring to the entire protein amount transferred. The results were quantitated by densitometry using Multi Gauge V3.2 software.

### Passive stiffness and Ca<sup>2+</sup>-sensitivity measurement

Force measurements were performed on single de-membrated cardiomyocytes ( $n = 10$ – $13$  cardiomyocyte/3–5 heart/group) as described before.<sup>29</sup> Briefly, LV samples were de-frozen in relaxing solution (containing in mM: 1.0 free Mg<sup>2+</sup>; 100 KCl; 2.0 EGTA; 4.0 Mg-ATP; 10 imidazole; pH 7.0), mechanically disrupted and incubated for 5 min in relaxing solution supplemented with 0.5% Triton X-100 (all from Sigma-Aldrich). The cell suspension was washed five times in relaxing solution. Single cardiomyocytes were selected under an inverted microscope (Zeiss Axiovert 135, 40 $\times$  objective; Carl Zeiss AG Corp, Oberkochen, Germany) and attached with shellac dissolved in ethanol between a force transducer and a high-speed length controller (piezoelectric motor) as part of a Myostretcher system (Ionoptix, Westwood, MA, USA). SL was monitored using a video camera, and analysis software was provided by the manufacturer.

Cardiomyocyte Ca<sup>2+</sup>-independent passive force ( $F_{\text{passive}}$ ) was measured in relaxing buffer at room temperature within a sarcomere length (SL) range between 1.8 and 2.3  $\mu$ m. Force values were normalized to myocyte cross-sectional area calculated from the diameter of the cells, assuming a circular shape. Cardiomyocyte  $F_{\text{passive}}$  was thereafter measured within a SL range between 1.8 and 2.3  $\mu$ m as described earlier. Then, the myocyte was adjusted to 2.2  $\mu$ m SL and exposed to a series of solutions with different pCa values ranging from 9.0 (relaxing) to 4.5 (maximal activation) to obtain the force-pCa relation. Force values were either related to maximum force at pCa 4.5 or normalized to myocyte cross-sectional area calculated from the diameter of the cells, assuming a circular shape. Mean values on relative force (and tension) versus pCa diagrams were fit with the 'Hill' equation, resulting in a sigmoidal curve.

## Statistical analysis

Data are expressed as the mean  $\pm$  SEM. The haemodynamic data of the animals, organ weights, functional parameters, plasma biomarkers, and western blot data were analysed with one-way ANOVA followed by Tukey *post hoc* test. A *P* value  $<0.05$  was accepted as statistically significant difference. \**P*  $<0.05$  4-month versus 8-month and #*P*  $<0.05$  Ctrl versus VO.

## Results

### Development of cardiac hypertrophy in volume overload rats with preserved ejection fraction

Transthoracic echocardiography was performed at the end of 4 and 8 months. The ejection fraction (EF) was preserved and unchanged between all groups (Figure 1B). Eight-month VO group showed increased left ventricular internal diameter

during diastole (LVID) (Figure 1C), additionally exhibited increased RV internal diameter (RVID) (Figure 1D), stroke volume (Figure 1E) and velocity-time index (Figure 1F) compared with their age-matched controls. However, there were no significant differences in mean arterial blood pressure (MABP) among all the groups (Figure 1G).

In this model, the body weights were significantly higher of the 8-month compared with the 4-month groups (Figure 2A). Because the body weight of both controls and VO was comparable at the same age, this indicates that the changes are age dependent. However, both 4- and 8-month VO exhibited significant increase in heart weights as compared with their aged-matched control groups (Figure 2B). Heart weight/body weight ratio was significantly elevated in both 4-month and 8-month VO animals as compared with their age-matched controls (Figure 2C). VO animals at 4- and 8-month showed a significant increase in LV (Figure 2D) RV weight (Figure 2E) as compared with the appropriate controls. The VO atrial weight at 8 months was significantly higher compared with all other groups (Figure 2F).

**Figure 2** Organ weights. (A) Animals' weights, (B) heart weights, (C) heart/body weight ratio, (D) left ventricular weights, (E) right ventricular weights, and (F) atria weights. Data are shown as mean  $\pm$  SEM; *n* = 5–6. \**P*  $<0.05$ . 4-month versus 8-month and #*P*  $<0.05$  Ctrl versus VO using one-way ANOVA Tukey multiple comparisons test.

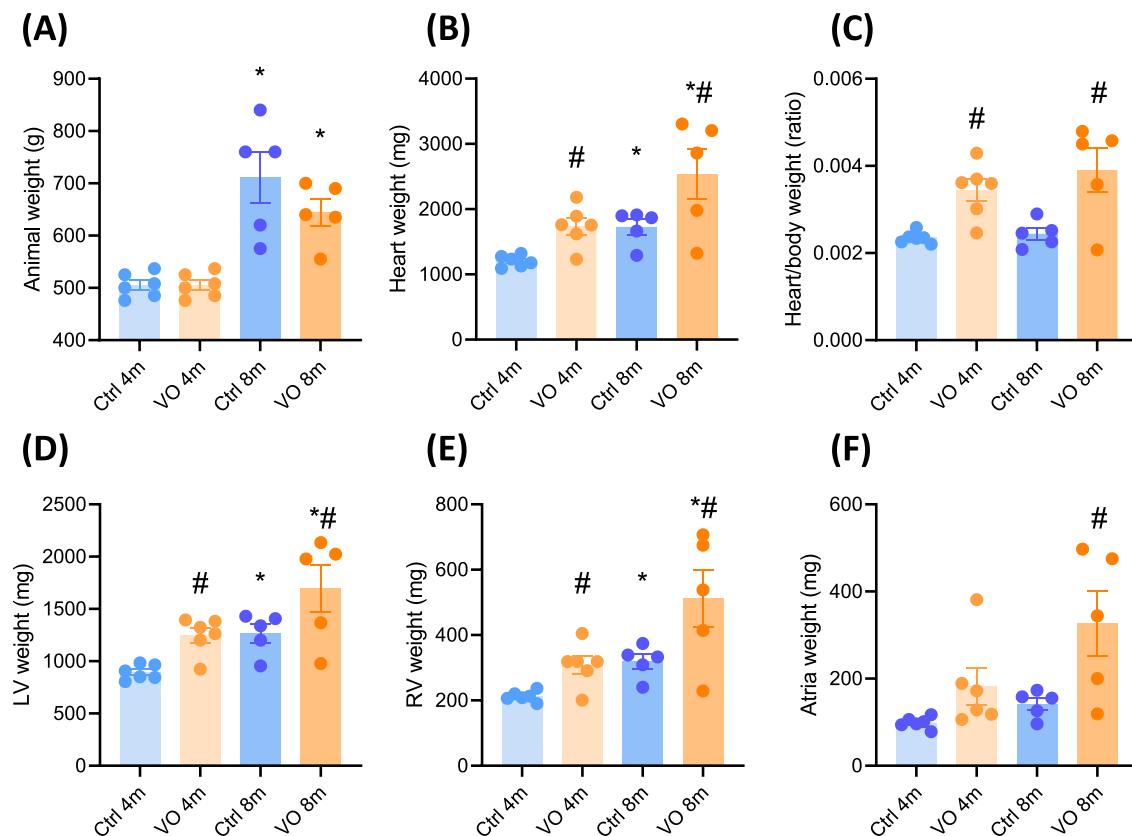
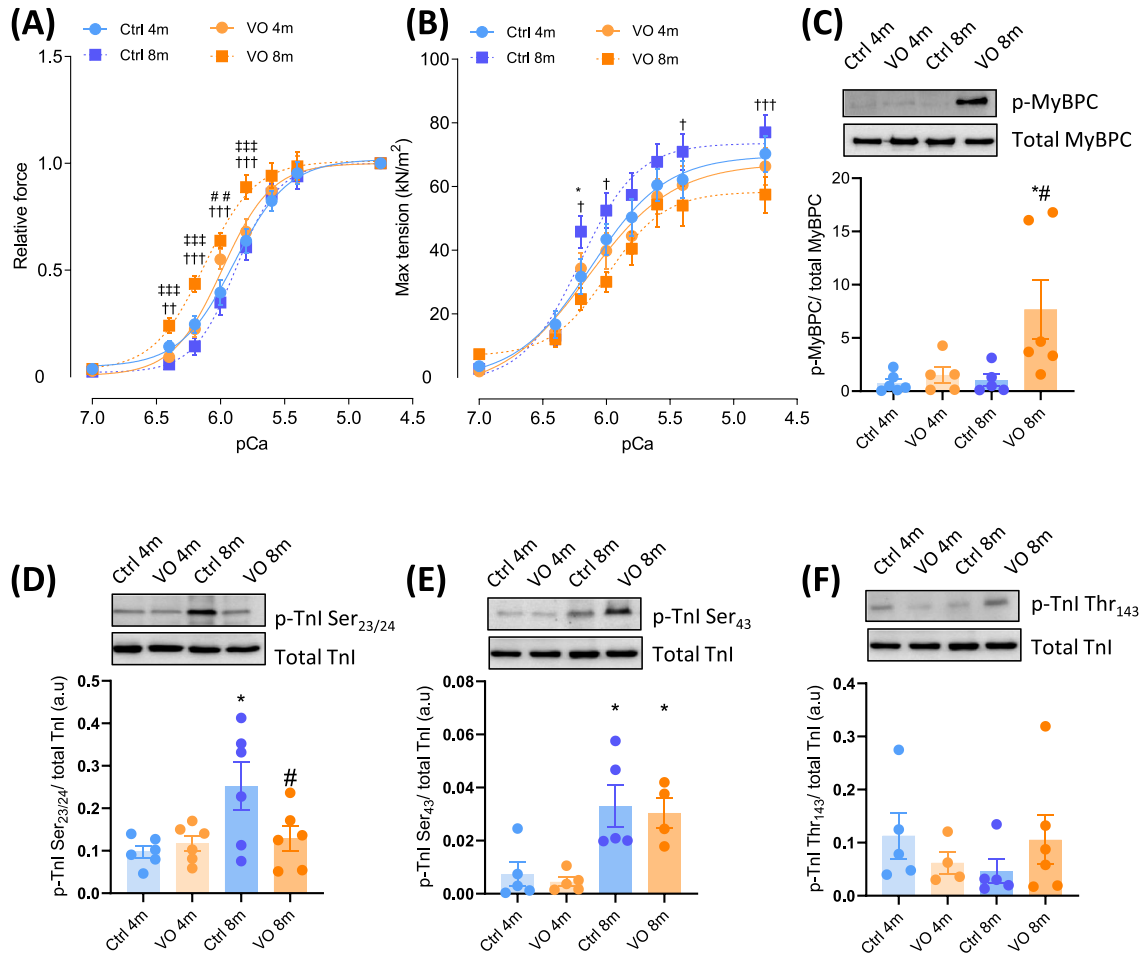


**Figure 3** Sarcomeric protein phosphorylation. (A) Calcium sensitivity, (B) maximum tension of sarcomere. Data are shown as mean  $\pm$  SEM;  $n = 5-6$ .  $n = 5-6$ .  $*P < 0.05$ . Ctrl 4-month versus 8-month;  $^{\dagger}P < 0.05/^{+++}P < 0.001$  Ctrl versus VO 8-month;  $^{+++}P < 0.001$  4-month versus 8-month VO; and  $\#P < 0.05$  Ctrl versus VO 4-month using one-way ANOVA Tukey multiple comparisons test. (C) Phosphorylation of cardiac myosin binding protein C level. (D) Site-specific phosphorylation of cTnI Ser<sub>23/24</sub>. (E) Site-specific phosphorylation of cTnI Ser<sub>43</sub>. (F) Site-specific phosphorylation of cTnI Thr<sub>143</sub>. Data are shown as mean  $\pm$  SEM;  $n = 5-6$ .  $*P < 0.05$  4-month versus 8-month,  $\#P < 0.05$  Ctrl versus VO using One way ANOVA Tukey multiple comparisons test.



### Impaired calcium sensitivity and myofilament proteins in VO animals

Ca<sup>2+</sup> sensitivity is an indicator of myofilament functional integrity, shifting to the left shows increased Ca<sup>2+</sup> sensitivity of tension. The force–pCa relationship of single skinned cardiomyocytes from 8-month VO revealed significantly higher myofilament Ca<sup>2+</sup> sensitivity (pCa<sub>50</sub>) compared with 4-month VO and control groups (Figure 3A). Furthermore, 4-month VO exhibited a slight leftward shift in force–pCa relations when compared with control groups, indicative of Ca<sup>2+</sup> sensitization as response to VO (Figure 3A). Maximum Ca<sup>2+</sup>-activated tension was significantly decreased in 8-month VO compared with its age-matched control group (Figure 3B).

cMyBPC phosphorylation was significantly higher in 8-month VO group (Figure 3C), after normalization to total cMyBPC level, which were unchanged between all groups. cTnI phosphorylation was investigated at three different phosphosites, normalized to the unchanged total cTnI expression level. At position Ser<sub>23/24</sub> (PKA- and PKG-dependent phosphorylation) phosphorylation was increased in 8-month control compared with 4-month control, but significantly lower in 8-month VO compared with 8-month control group and 8-month VO were unchanged compared with 4-month VO, indicating hypophosphorylation of cTnI Ser<sub>23/24</sub> and thereby contributing to the elevated Ca<sup>2+</sup> sensitivity in 8-month VO (Figure 3D). Site-specific phosphorylation of cTnI at Ser<sub>43</sub> position (PKC-dependent phosphorylation) was significantly higher in both 8-month control and VO groups com-

pared with the 4-month respective groups (Figure 3E), while PKC phosphosite at residue Thr<sub>143</sub> was unchanged among all groups (Figure 3F).

### Increased titin-based myocardial stiffness and altered titin phosphorylation in VO animals

Elevated myocardial stiffness is associated with hypertrophic cardiac remodelling.<sup>30</sup> Titin's mechanosensing function and its posttranslational modifications are central determinants of cardiomyocyte stiffness.<sup>12</sup> Hence, we measured in skinned cardiomyocytes the Ca<sup>2+</sup>-independent  $F_{\text{passive}}$  within SL ranging between 1.8 and 2.4  $\mu\text{m}$ . We found  $F_{\text{passive}}$  of 8-month VO cardiomyocytes to be significantly elevated at SL 2.0–2.4  $\mu\text{m}$  compared with all other groups (Figure 4A), suggesting VO-dependent alterations in titin-based myocardial stiffness. Of note, 8-month control cardiomyocytes exhibited a significant increase in  $F_{\text{passive}}$  at SL 2.2–2.3  $\mu\text{m}$  as compared with 4-month control group, which can potentially result from aging-related myocardial changes; however, the 4-month VO showed the same elevated  $F_{\text{passive}}$  as 8-month control, indicating VO dependency.

Along with the changes of the  $F_{\text{passive}}$ , total titin phosphorylation was significantly reduced in both 4- and 8-month VO groups (Figure 4B). Additionally, we detected altered phosphorylation of specific residues within the unique sequence of the elastic spring region N2Bus and PEVK region of titin.

Despite the overall hypophosphorylation of titin in 4- and 8-month VO, the CaMKII-dependent phosphorylation at Ser<sub>4043</sub> in the N2Bus was significantly increased when compared with the age-matched control groups (Figure 4C). Furthermore, we looked at the site-specific phosphorylation within the PEVK region of titin. We found that CaMKII-dependent phosphorylation at Ser<sub>12884</sub> was also elevated in both 4- and 8-month VO compared with age-matched control groups (Figure 4D). This was in line with increased oxidation of CaMKII in both 4- and 8-month VO as compared with the control groups (Figure 4E), while the expression levels (Figure 4F) and autophosphorylation (Figure 4G) were unchanged between the groups.

We found that PKG-dependent Ser<sub>4080</sub> conserved phosphosites were hypophosphorylated in both 4- and 8-month VO groups as compared with the age-matched controls, respectively (Figure 5A). Polymerization of PKG is observed upon oxidation during oxidative stress. A representative image in Figure 5B shows the monomer, dimer, and polymer PKG signal intensities. Results show elevated amounts of dimer PKG in volume overload groups as compared with the age-matched controls (Figure 5C). Monomeric PKG was significantly reduced in 4- and 8-month VO compared with the control groups (Figure 5D). Dimerization of PKG was significantly elevated in 8-month VO group (Figure 5E). PKG polymers showed significantly elevated amount not only in comparison with VO

and control groups, but also regarding time, in comparison with 4-month to 8-month groups (Figure 5F).

### Alteration of signalling pathways due to volume overload

As titin is phosphorylated by numerous kinases including CaMKII and PKG (Figures 4 and 5) that modulate the titin stiffness, we also looked at other potential kinases that can be modulated upon hypertrophy. PKA phosphosite on titin N2Bus region, at Ser<sub>3991</sub>, showed hypophosphorylation both at 4- and 8-month VO groups as compared with the controls (Supporting Information, Figure S1A), while PKA expression level did not show any change (Supporting Information, Figure S1B) among the groups. PKC $\alpha$  specific phosphosite at PEVK region, at Ser<sub>12742</sub> showed no differences among groups (Supporting Information, Figure S1C), while PKC $\alpha$  expression was significantly higher in 8-month VO (Supporting Information, Figure S1D), indicating an increased PKC $\alpha$  activity in 8-month VO.

Finally, based on its role in hypertrophic remodelling and involvement in cardiomyocyte dysfunction and also its ability to phosphorylate titin, we investigated the expression level of mitogen-activated protein kinase (MAPK, also known as extracellular signal-regulated kinases, ERK1 and 2). Expression level of MAPK were unchanged (Supporting Information, Figure S1E,G); however, the phosphorylation of MAPK detected at the molecular weight 42 kDa was significantly increased in 8-month compared with 4-month VO (Supporting Information, Figure S1F). The phosphorylation of the 44 kDa MAPK isoform showed slightly, but non-significant changes in 8-month groups (Supporting Information, Figure S1H).

## Discussion

The current study showed that 8-month VO rat model developed cardiac hypertrophy with preserved ejection fraction in response to volume overload associated with alterations in myofilament proteins phosphorylation due to changes in CaMKII and PKG signalling pathways. These changes were mainly caused by alterations in the oxidative status of CaMKII and PKG and contributing by this to cardiomyocyte dysfunction as depicted from modulation of calcium sensitivity, maximal generated tension, and titin-based stiffness. This finding shows for the first time how oxidation of CaMKII and PKG could contribute to sarcomeric dysfunction in early model of hypertrophy, suggesting a potential therapeutic targets for those with early stage of hypertrophy.



**Figure 4** Titin-based myocardial stiffness and titin phosphorylation by CaMKII. (A) Passive tension-sarcomere length relations of control (Ctrl) and volume overload (VO) cardiomyocytes at sarcomere length (SL) 1.8–2.4  $\mu$ M. All force recordings were normalized for cardiomyocyte cross-sectional area. Curves represent third order polynomial regressions.  $**P < 0.01$ / $***P < 0.001$ . Ctrl 4-month versus 8-month;  $\dagger P < 0.05$ / $\dagger\dagger\dagger P < 0.001$  Ctrl versus VO 8-month;  $\ddagger P < 0.01$ / $\ddagger\ddagger\ddagger P < 0.001$  4-month versus 8-month VO; and  $\#P < 0.05$ / $\#\#\# P < 0.01$  Ctrl versus VO 4-month using one-way ANOVA Tukey multiple comparisons test. (B) Overall titin and (E–G) CaMKII-specific phosphorylation measurement by western immunoblots from left ventricular tissue. Representative blots show antibody staining at position (C) Ser<sub>4043</sub> (N2Bus) and (D) Ser<sub>12884</sub> (PEVK). PVDF stains are included for comparisons of loading (E) oxidation of CaMKII, (F) CaMKII expression level, (G) phosphorylation of CaMKII at Thr<sub>286</sub>. Data are shown as mean  $\pm$  SEM;  $n = 4$ .  $\#P < 0.05$  Ctrl versus VO using one-way ANOVA Tukey multiple comparisons test.

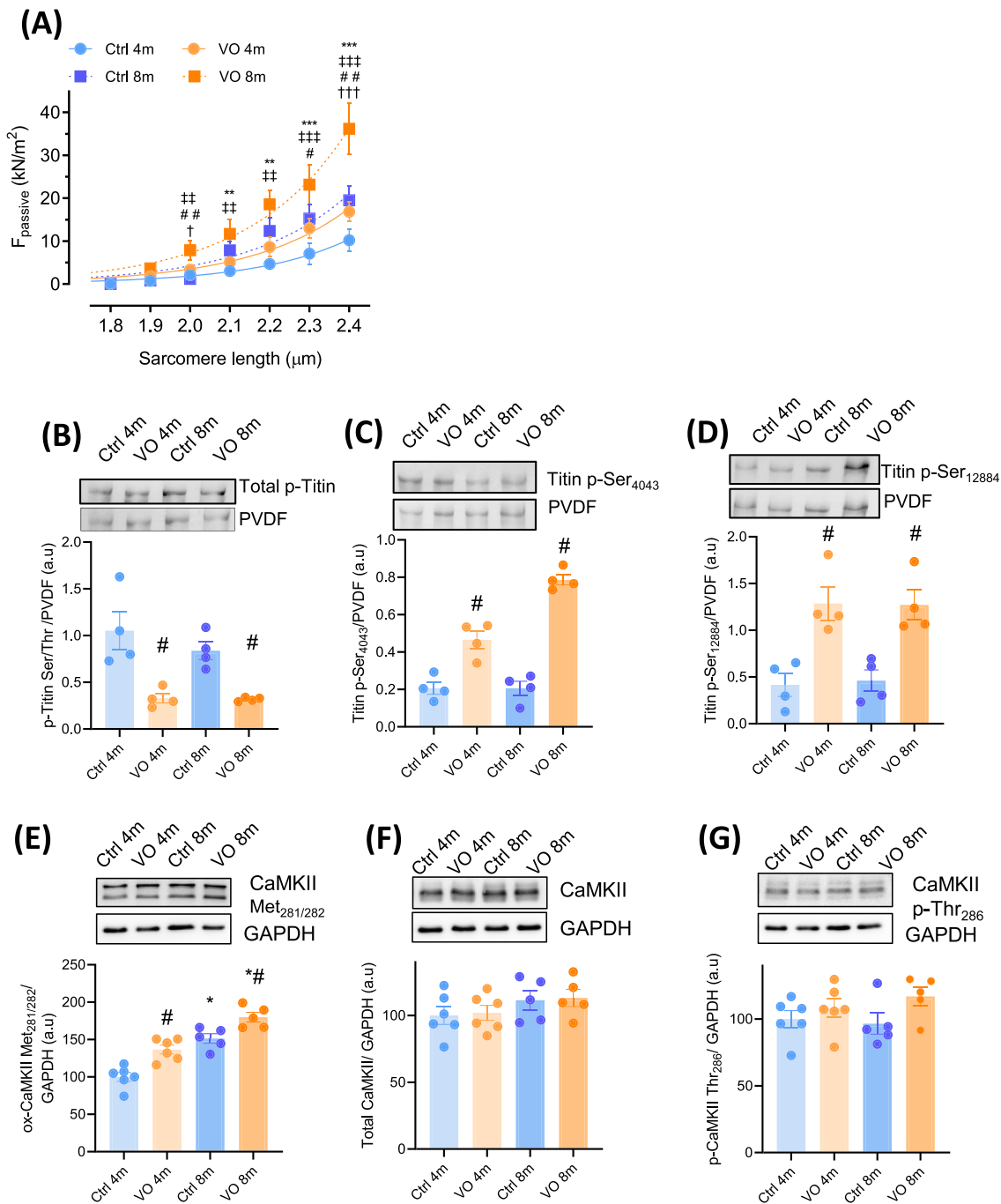
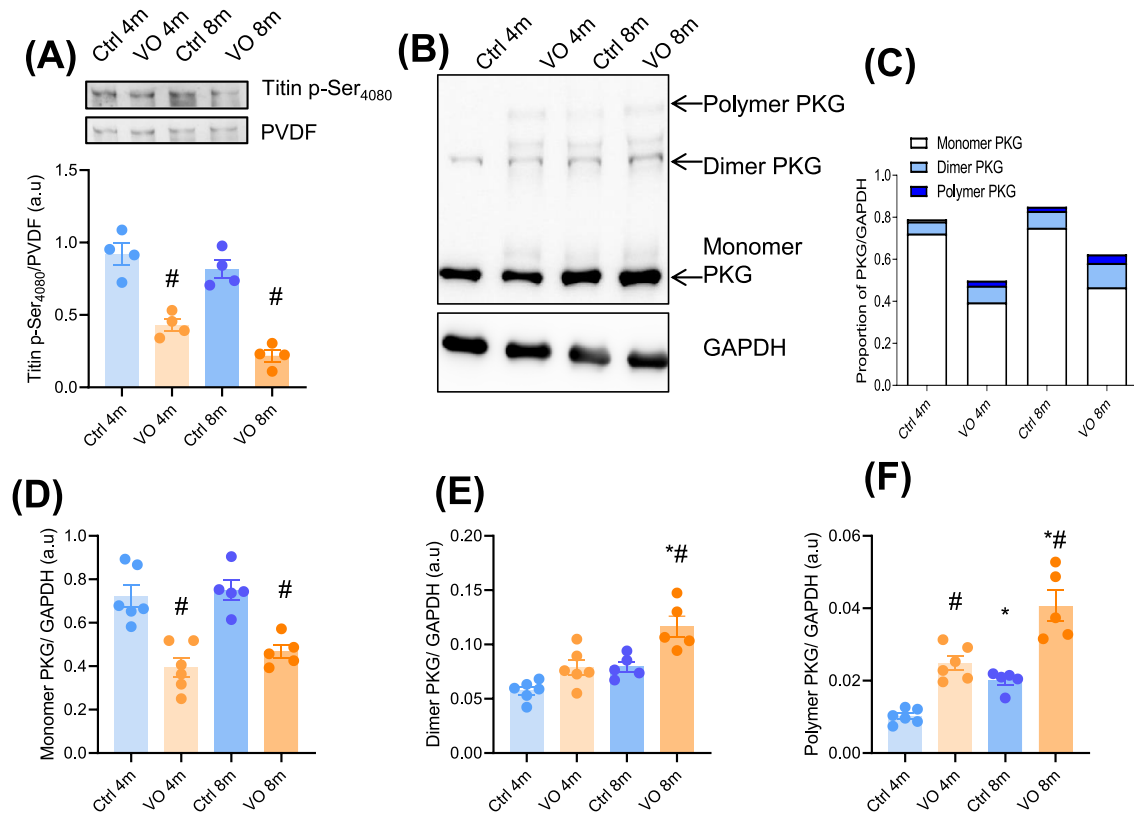


**Figure 5** Titin phosphorylation by PKG. (A) Titin phosphorylation at Ser<sub>4080</sub> (N2Bus), (B) representative blot of PKG levels. (C) Distribution of PKG isoforms, (D) monomer level of PKG, (E) dimer level of PKG, (F) polymer level of PKG. Data are shown as mean  $\pm$  SEM;  $n = 5-6$ . # $P < 0.05$  Ctrl versus VO. \* $P < 0.05$  4-month versus 8-month using one-way ANOVA Tukey multiple comparisons test.



## Altered phosphorylation status of sarcomeric proteins and myofilament Ca<sup>2+</sup> sensitivity in VO

Pathological and pathophysiological alterations have been reported in VO models.<sup>1,31</sup> Earlier, in compensated stages, alterations in myofilament Ca<sup>2+</sup> sensitivity, cross-bridge cycling, and electromechanical coupling across the intercalated disc have been documented,<sup>32</sup> in addition to alterations in Ca<sup>2+</sup> cycling at the late stages of VO induced HF progression in rats, dogs, and humans.<sup>32-35</sup> However, the changes of sarcomeric proteins remain at end-stage heart failure, even without a significant change in the amount of Ca<sup>2+</sup> available for contraction. In agreement with these studies, our model showed changes in the myofilament Ca<sup>2+</sup> sensitivity and maximal tension; both were associated with myofilament proteins phosphorylation deficit. Previously, it has been shown that these changes could also be associated with alterations in myofibrillar ATPase activity<sup>36,37</sup> and/or the allosteric effect of the troponin complex, which may also contribute to Ca<sup>2+</sup> sensitivity changes.<sup>38</sup> Several studies suggested that the difference in Ca<sup>2+</sup> responsiveness in the failing heart is not reflected in intrinsic differences in the protein isoform com-

position or expression,<sup>39-41</sup> likewise in the presented model, we did not find any differences in the expression level of the myofilament proteins, but rather changes in the endogenous phosphorylation level. Deranged phosphorylation of myofilament proteins seen in HF patients and animal models of HF was most of the time associated with increased and reduced activity of CaMKII and PKG, respectively.<sup>22,25</sup> In addition to increased CaMKII and PKG oxidation<sup>26,42</sup> in both, this could contribute to observed myofilament phosphorylation dysregulation and thereby hypertrophy.

Myofilament Ca<sup>2+</sup> sensitivity is highly modulated by the phosphorylation status of sarcomeric proteins such as cTnI and cMyBPC. Both contain multiple phosphorylation sites that are targeted by several kinases including PKA, PKG, PKD, and CaMKII. Hence, the net effect of myofilament sensitization/desensitization is defined by synergistic balance between different kinases/phosphatases.<sup>9,14</sup> In the current study, and in line with previous work reporting the reduction in PKA-dependent phosphorylation of cTnI in end stage human failing hearts,<sup>19,43,44</sup> we found PKA/PKG-dependent hypophosphorylation of cTnI at Ser<sub>23/24</sub> in 8-month VO compared with 8-month Ctrl group. It is well established that in

HF and due to the internalization of  $\beta$ -adrenergic receptors, the receptor density and activity are reduced leading to decreased PKA-dependent phosphorylation of cTnI at Ser<sub>23/24</sub>.<sup>44</sup> This might explain the elevated Ca<sup>2+</sup> sensitivity of skinned cardiomyocytes from 8-month VO group, despite the unchanged PKA expression level; however, we cannot exclude the possibility of reduced PKA enzyme activity in the 8-month VO rats. We observed cTnI hyperphosphorylation at Ser<sub>43</sub> (PKC-dependent phosphorylation) in both 8-month VO and Ctrl groups. Previous studies reported that increased PKC activity has a maladaptive effect on sarcomeric function in HF and suggested the beneficial effect of reducing the Ser<sub>43</sub> phosphorylation on the cardiomyocyte function.<sup>45</sup> Moreover, reduced PKA-dependent phosphorylation of cMyBPC is also associated with myofilament Ca<sup>2+</sup> sensitization, impaired relaxation, and hypertrophic remodelling.<sup>19,43,46,47</sup> However, our data showed significant increase in the total phosphorylation of cMyBPC in 8-month VO which might also contribute to the modulation of myofilament Ca<sup>2+</sup> sensitivity as reported before.<sup>22</sup> This finding could be explained by the fact that cMyBPC is additionally targeted by PKG, PKC and CaMKII.<sup>48</sup> The latter was suggested to facilitate the phosphorylation of the two PKA sites on cMyBPC.<sup>7,15</sup> In summary, hypo- and hyperphosphorylation of regulatory myofilament proteins and increased Ca<sup>2+</sup> sensitivity in 8-month VO indicates that functional impairment at sarcomeric level could be an early event in the development of HF. Of note, the altered myofilament Ca<sup>2+</sup> sensitivity has been suggested to be an early compensatory response to pressure overload.<sup>49</sup> A key mediator in this process is the disturbed Ca<sup>2+</sup> homeostasis and the subsequent activation of CaMKII leading to CaMKII mediated maladaptive hypertrophy.<sup>50</sup> Similar effect may therefore be predicted upon VO. Hence, we focused on the contribution of CaMKII to the initiation of VO-induced cardiac hypertrophy.

### Increased titin-based myocardial stiffness and the role of CaMKII and PKG oxidation in VO

HF is often accompanied by increased titin-based myocardial stiffness.<sup>12</sup> Hypertrophy and stretch are also associated with alterations in titin spring elements.<sup>51</sup> Different structural proteins show changes in their expression in different HF causes, phenotypes, and stages. Titin is a huge interface molecule that plays a key role in the assembly of structural and regulatory proteins of the cardiomyocyte, determining by these the active and passive mechanical properties of the sarcomere.<sup>12,13,52</sup> The physiological function of titin implies that alterations in titin expression or the isoform switch may contribute to depressed contractility in failing human heart and animal models of HF,<sup>12,53–55</sup> more elastic titin isoform represents an adaptation to the increased wall stiffness of the heart.<sup>41</sup>

Our model showed global titin phosphorylation deficit associated with CaMKII-dependent site specific hyperphosphorylation. Various CaMKII-dependent titin phospho-sites were detected by quantitative mass spectrometry (MS), some of which are located within the extensible region of titin at the N2Bus and PEVK spring elements and some within the A-band, M-band, and Z-disk of titin.<sup>18</sup> CaMKII-mediated titin phosphorylation reduces cardiomyocyte F<sub>passive</sub>.<sup>18</sup> Although phospho-site Ser<sub>4043</sub> (CaMKII-dependent phosphorylation) was increased in the 8-month VO, the cardiomyocyte F<sub>passive</sub> persists to be elevated, perhaps due to increased CaMKII oxidation, suggesting that CaMKII post-translational modification may contribute to the increase in its activity<sup>18,56</sup> and thereby partially contributing to the elevated F<sub>passive</sub> in 8-month VO. Indeed, it has been evident that oxidation of Met<sub>281/282</sub> in the regulatory domain of CaMKII induces an autonomous-Ca<sup>2+</sup>/CaM-independent activation.<sup>20,21,57</sup> Hyperactivation of CaMKII was reported as maladaptive response in patients and animal models of HF.<sup>58,59</sup> The pathological responses to ROS-induced CaMKII hyperactivation include atrial fibrillation, stemming from diastolic sarcoplasmic reticulum Ca<sup>2+</sup> leakage (due to a hyperphosphorylation of the RyR2 at Ser<sub>2815</sub>).<sup>60</sup> Moreover, hypertrophic remodelling, inflammation, and apoptosis were shown to follow CaMKII-dependent phosphorylation of histone deacetylase 4 (HDAC4), thereby promoting the up-regulation of the fetal cardiac gene expression such as the myocyte enhancer factor-2 (MEF2) and the nuclear factor kappa-light-chain-enhancer of activated B cells (NF- $\kappa$ B).<sup>61–63</sup> Furthermore, CaMKII inhibition via peptides or ant-oxidants was reported to be beneficial in cardiovascular diseases.<sup>64</sup> The maladaptive responses to CaMKII hyperactivation are mostly driven by the deranged phosphorylation of its downstream targets such as ion channels, Ca<sup>2+</sup> homeostatic proteins, and sarcomeric proteins.<sup>18,65</sup> The latter finding is supported by our current and previous work indicating the contribution of sarcomeric dysfunction upon phosphorylation deficit of myofilament proteins in particular the giant protein titin.<sup>18,26,54,56</sup>

Growing evidence demonstrates the pivotal role of nitric oxide-soluble guanylyl cyclase- cyclic guanosine monophosphate-PKG (NO-sGC-cGMP-PKG) signalling cascade in cardiac diseases. PKG phosphorylates N2Bus spring element in titin, thereby reduces titin-based myocardial stiffness.<sup>12</sup> Previous work reported the important contribution of oxidative activation of PKG I $\alpha$  independently from the NO-cGMP pathway.<sup>66,67</sup> Burgoyne *et al.* demonstrated that H<sub>2</sub>O<sub>2</sub> exposure induces the formation of disulphide bond between the 2  $\alpha$  subunits of PKG which facilitates its activation in the absence of cGMP.<sup>66</sup> In contrast, other studies showed that C42 oxidation reduces PKGI $\alpha$ 's activation capacity to counter hormone, haemodynamic, and cardiotoxic stress.<sup>68,69</sup> Furthermore, C42 oxidation has been linked to an amplified the mammalian (mechanistic) target of rapamycin complex 1

(mTORC1) activity and depressed autophagy in PO-induced hypertrophy.<sup>70</sup> Previously, we showed that oxidative stress and inflammation arising from several cardiovascular co-morbidities diminished NO bioavailability and led to the attenuation of cGMP-PKG signalling, hypophosphorylation of N2Bus element in titin, and elevated cardiomyocyte stiffness in HFpEF and hypertrophic cardiomyopathy (HCM) patients.<sup>19,25,71</sup> *Ex vivo* administration of PKA and cGMP-dependent PKG corrected all-titin phosphorylation deficit in human and animal models of HF and reduced thereby the pathologically increased titin-based stiffness observed in human and animal model with HF.<sup>19,25,71</sup> Accordingly, the VO groups showed increased cardiomyocyte stiffness in line with titin phosphorylation deficit which was associated with PKG oxidation. PKG-mediated phosphorylation of titin results in acutely increased cardiac distensibility following short-term cGMP-enhancing treatment with sildenafil and BNP in an HFpEF animal model.<sup>72</sup> Interestingly, the sodium glucose cotransporter 2 inhibitors (SGLT2i) improved the inflammatory and oxidative stress in human and rat HFpEF myocardium, which improved NO-sGC-cGMP-PKG cascade and directly enhanced PKG $\alpha$  activity via reduced PKG $\alpha$  oxidation. Consequently, pathological cardiomyocyte function in human HFpEF myocardium was reversible by SGLT2i via improved PKG $\alpha$  and the anti-oxidative effect of SGLT2i.<sup>26</sup>

### Dysregulation of titin phosphorylation by PKA and MAPK in VO

Both PKA and PKC target N2Bus or PEVK titin segments and lead to a decrease or an increase in cardiomyocyte stiffness, respectively.<sup>73</sup> We found PKA-dependent hypophosphorylation at Ser<sub>3991</sub> within N2Bus-titin, which might contribute to elevated passive stiffness measured in 8-month VO. The PKC $\alpha$ -dependent phosphorylation at Ser<sub>12742</sub> within the PEVK-titin segment was unchanged, indicating to the substantial contribution of PKG and CaMKII oxidation to the elevated myocyte stiffness in 8-month VO model and a potential synergy between the two kinases.

Another kinase that phosphorylates titin is the MAPK which phosphorylates titin at the N2B spring element. Although the mechanical effects of this phosphorylation still need to be more firmly established, MAPK is an effector kinase of the rapidly accelerated fibrosarcoma 1 (Raf1)-MEK1/2-MAPK pathway and has been implicated in cardiac hypertrophy.<sup>74</sup> Hence, our findings suggest that MAPK activity is increased as appreciated from increased MAPK phosphorylation. Therefore, MAPK may also contribute to elevated passive stiffness measured in 8-month VO. Taken together, these findings underscore the importance of titin

phosphorylation changes for cardiomyocyte F<sub>passive</sub> in volume overload induced hypertrophy.

### Altered hypertrophic signalling in VO

In addition to altered phosphorylation status of sarcomeric proteins, disturbed kinases signalling is involved in multiple pathways responsible for hypertrophic growth.<sup>30</sup> NO-cGMP-PKG pathway was shown to suppress cardiac hypertrophy by inhibiting calcineurin-NFAT signalling.<sup>75</sup> PKG oxidation is also involved in the modulation of mTOR signalling in PO-induced hypertrophy.<sup>70</sup> Therefore, its down-regulation might contribute to hypertrophic remodelling.<sup>75</sup> Furthermore, coordination of MAPK and NFAT signalling regulates the hypertrophic response. Phosphorylated NFAT causes inhibition of its nuclear translocation and thus attenuating cardiac hypertrophy and thereby contributing to regulation of the hypertrophic response.<sup>75</sup> Hence, impaired hypertrophic signalling might add to the cardiac remodelling and mechanical dysfunction in early stage of VO induced hypertrophy.

### Conclusion

In this work, we report the early pathological response to VO, which manifests in cardiomyocyte mechanical disturbances and dysfunction. Our data demonstrate the elevation in Ca<sup>2+</sup> sensitivity and titin-based cardiomyocyte stiffness in 8-month VO model, mainly due to CaMKII and PKG oxidation. The modulation of these two kinases contributed to deranged phosphorylation of sarcomeric proteins that are involved in cardiac contractility and relaxation. In line with our conclusion, it has been previously reported that VO associates with several pathological events including oxidative stress and inflammatory response.<sup>76,77</sup> Therefore, we believe that our model exhibits an increase of oxidative stress and inflammation, which requires further investigations. Previous work by us and others demonstrated the role of oxidative-stress induced modulation of kinase activity and affinity to their substrates.<sup>19,78</sup> Hence, we cannot rule out oxidative-stress mediated alterations in sarcomeric proteins structure and stability,<sup>19,30</sup> which awaits further investigation. In summary, our study highlights the adverse consequences of CaMKII and PKG oxidation on cardiomyocyte function in the early stage of VO-induced cardiac hypertrophy. These findings may provide critical insight into how to prevent or decelerate the development of HF development and progression potentially via reduced oxidative stress and thereby preventing CaMKII and PKG oxidation. This may reverse deranged myofilament phosphorylation and thereby improve cardiomyocyte function.

## Conflict of interest

P.F. is the founder and CEO, and A.G. is involved in the management of Pharmahungary Group, a group of R&D companies.

## Funding

The project has received funding from the EU's Horizon 2020 research and innovation program under grant agreement No. 739593 to NH; DFG (Deutsche Forschungsgemeinschaft) HA 7512/2-4 and HA 7512/2-1 to NH; NRD Fund 2019-1.1.1-PIACI-KFI-2019-00367; Thematic Excellence Programme 2020-4.1.1.-TKP2020; New National Excellence Program UNKP-21-5-SZTE-543; János Bolyai Research Fellowship of the Hungarian Academy of Sciences bo\_481\_21; EMBO short-term fellowship 8792 Heinrich und Alma Vogelsang

Stiftung; German Academic Exchange Service (DAAD); European HCEMM HU26307383; Hungarian National Scientific Research Fund OTKA-138223, K139237.

## Supporting information

Additional supporting information may be found online in the Supporting Information section at the end of the article.

**Figure S1.** Kinase activities from left ventricle tissue. **A)** Phosphorylation of titin at Ser<sub>3991</sub> (N2Bus), **B)** Expression level of PKA **C)** Phosphorylation of titin at Ser<sub>12742</sub> (PEVK) **D)** Protein kinase C $\alpha$  expression level, **E)** MAPK expression level (42 kDa) **F)** phospho-MAPK (42 kDa) **G)** MAPK expression level (44 kDa) **H)** Phospho-MAPK (44 kDa). Data are shown as mean $\pm$ SEM; n = 5–6. #P < 0.05 Ctrl vs. VO. \*P < 0.05 4-month vs 8-month using One way ANOVA Tukey multiple comparisons test.

## References

- Pitoulis FG, Terracciano CM. Heart plasticity in response to pressure- and volume-overload: A review of findings in compensated and decompensated phenotypes. *Front Physiol.* 2020; **11**: 92.
- Schnelle M, Sawyer I, Anilkumar N, Mohamed BA, Richards DA, Toischer K, Zhang M, Catibog N, Sawyer G, Mongue-Din H, Schröder K, Hasenfuss G, Shah AM. NADPH oxidase-4 promotes eccentric cardiac hypertrophy in response to volume overload. *Cardiovasc Res.* 2021; **117**: 178–187.
- van Heerebeek L, Borbely A, Niessen HW, Borbely A, Bronzwaer JGF, van der Velden J, Stienen GJM, Linke WA, Laarman GJ, Paulus WJ. Myocardial structure and function differ in systolic and diastolic heart failure. *Circulation.* 2006; **113**: 1966–1973.
- Zhazykbayeva S, Pabel S, Mugge A, Sossalla S, Hamdani N. The molecular mechanisms associated with the physiological responses to inflammation and oxidative stress in cardiovascular diseases. *Biophys Rev.* 2020; **12**: 947–968.
- Kobayashi T, Solaro RJ. Calcium, thin filaments, and the integrative biology of cardiac contractility. *Annu Rev Physiol.* 2005; **67**: 39–67.
- You J, Wu J, Zhang Q, Ye Y, Wang S, Huang J, Liu H, Wang X, Zhang W, Bu L, Li J, Lin L, Ge J, Zou Y. Differential cardiac hypertrophy and signaling pathways in pressure versus volume overload. *Am J Physiol Heart Circ Physiol.* 2018; **314**: H552–H562.
- Gautel M, Zuffardi O, Freiburg A, Labelle S. Phosphorylation switches specific for the cardiac isoform of myosin binding protein-C: A modulator of cardiac contraction? *EMBO J.* 1995; **14**: 1952–1960.
- Jia W, Shaffer JF, Harris SP, Leary JA. Identification of novel protein kinase A phosphorylation sites in the M-domain of human and murine cardiac myosin binding protein-C using mass spectrometry analysis. *J Proteome Res.* 2010; **9**: 1843–1853.
- Solaro RJ, van der Velden J. Why does troponin I have so many phosphorylation sites? Fact and fancy. *J Mol Cell Cardiol.* 2010; **48**: 810–816.
- Mohamed AS, Dignam JD, Schlender KK. Cardiac myosin-binding protein C (MyBP-C): Identification of protein kinase A and protein kinase C phosphorylation sites. *Arch Biochem Biophys.* 1998; **358**: 313–319.
- Hartzell HC, Glass DB. Phosphorylation of purified cardiac muscle C-protein by purified cAMP-dependent and endogenous Ca<sup>2+</sup>-calmodulin-dependent protein kinases. *J Biol Chem.* 1984; **259**: 15587–15596.
- Linke WA, Hamdani N. Gigantic business: Titin properties and function through thick and thin. *Circ Res.* 2014; **114**: 1052–1068.
- Hamdani N, Herwig M, Linke WA. Tampering with springs: Phosphorylation of titin affecting the mechanical function of cardiomyocytes. *Biophys Rev.* 2017; **9**: 225–237.
- Salhi HE, Hassel NC, Siddiqui JK, Brundage EA, Ziolo MT, Janssen PML, Davis JP, Biesiadecki BJ. Myofilament calcium sensitivity: Mechanistic insight into TnI Ser-23/24 and Ser-150 phosphorylation integration. *Front Physiol.* 2016; **7**: 567.
- McClellan G, Kulikovskaya I, Winegrad S. Changes in cardiac contractility related to calcium-mediated changes in phosphorylation of myosin-binding protein C. *Biophys J.* 2001; **81**: 1083–1092.
- van der Velden J, Narolska NA, Lamberts RR, Vandervelden J, Narolska N, Lamberts R, Boontje N, Borbely A, Zaremba R, Bronzwaer J, Papp Z, Jaquet K, Paulus W. Functional effects of protein kinase C-mediated myofilament phosphorylation in human myocardium. *Cardiovasc Res.* 2006; **69**: 876–887.
- Kirchhefer U, Schmitz W, Scholz H, Neumann J. Activity of cAMP-dependent protein kinase and Ca<sup>2+</sup>/calmodulin-dependent protein kinase in failing and nonfailing human hearts. *Cardiovasc Res.* 1999; **42**: 254–261.
- Hamdani N, Krysiak J, Kreusser MM, Neef S, dos Remedios CG, Maier LS, Krüger M, Backs J, Linke WA. Crucial role for Ca<sup>2+</sup>/calmodulin-dependent protein kinase-II in regulating diastolic stress of normal and failing hearts via titin phosphorylation. *Circ Res.* 2013; **112**: 664–674.
- Budde H, Hassoun R, Tangos M, Zhazykbayeva S, Herwig M,

- Varatnitskaya M, Sieme M, Delalat S, Sultana I, Kolijn D, Gömöri K, Jarkas M, Lódi M, Jaquet K, Kovács Á, Mannherz HG, Sequeira V, Mügge A, Leichert LI, Sossalla S, Hamdani N. The interplay between S-Glutathionylation and phosphorylation of cardiac troponin I and myosin binding protein C in end-stage human failing hearts. *Antioxidants (Basel)*. 2021; **10**: 1134.
20. Erickson JR. Mechanisms of CaMKII activation in the heart. *Front Pharmacol*. 2014; **5**: 59.
  21. Mollova MY, Katus HA, Backs J. Regulation of CaMKII signaling in cardiovascular disease. *Front Pharmacol*. 2015; **6**: 178.
  22. Hamdani N, Bishu KG, von Frieling-Salewsky M, Redfield MM, Linke WA. Deranged myofilament phosphorylation and function in experimental heart failure with preserved ejection fraction. *Cardiovasc Res*. 2013; **97**: 464–471.
  23. Hofmann F, Wegener JW. cGMP-dependent protein kinases (cGK). *Methods Mol Biol*. 2013; **1020**: 17–50.
  24. Dunkerly-Eyring B, Kass DA. Myocardial Phosphodiesterases and their role in cGMP regulation. *J Cardiovasc Pharmacol*. 2020; **75**: 483–493.
  25. Kolijn D, Kovacs A, Herwig M, Kovács Á, Lódi M, Sieme M, Alhaj A, Sandner P, Papp Z, Reusch PH, Haldenwang P, Falcão-Pires I, Linke WA, Jaquet K, van Linthout S, Mügge A, Tschöpe C, Hamdani N. Enhanced cardiomyocyte function in hypertensive rats with diastolic dysfunction and human heart failure patients after acute treatment with soluble guanylyl cyclase (sGC) activator. *Front Physiol*. 2020; **11**: 345.
  26. Kolijn D, Pabel S, Tian Y, Lódi M, Herwig M, Carrizzo A, Zhazykbayeva S, Kovács Á, Fülöp GÁ, Falcão-Pires I, Reusch PH, Linthout SV, Papp Z, van Heerebeek L, Vecchione C, Maier LS, Ciccarelli M, Tschöpe C, Mügge A, Bagi Z, Sossalla S, Hamdani N. Empagliflozin improves endothelial and cardiomyocyte function in human heart failure with preserved ejection fraction via reduced pro-inflammatory-oxidative pathways and protein kinase Galpha oxidation. *Cardiovasc Res*. 2021; **117**: 495–507.
  27. Hamdani N, Franssen C, Lourenco A, Lourenço A, Falcão-Pires I, Fontoura D, Leite S, Plettig L, López B, Ottenheijm CA, Becher PM, González A, Tschöpe C, Díez J, Linke WA, Leite-Moreira AF, Paulus WJ. Myocardial titin hypophosphorylation importantly contributes to heart failure with preserved ejection fraction in a rat metabolic risk model. *Circ Heart Fail*. 2013; **6**: 1239–1249.
  28. Michel K, Herwig M, Werner F, Špiranec Spes K, Abeßer M, Schuh K, Dabral S, Mügge A, Baba HA, Skryabin BV, Hamdani N, Kuhn M. C-type natriuretic peptide moderates titin-based cardiomyocyte stiffness. *JCI Insight*. 2020; **5**: e139910.
  29. Loescher CM, Breitzkreuz M, Li Y, Nickel A, Unger A, Dietl A, Schmidt A, Mohamed BA, Kötter S, Schmitt JP, Krüger M, Krüger M, Toischer K, Maack C, Leichert LI, Hamdani N, Linke WA. Regulation of titin-based cardiac stiffness by unfolded domain oxidation (UnDOx). *Proc Natl Acad Sci U S A*. 2020; **117**: 24545–24556.
  30. Hassoun R, Budde H, Zhazykbayeva S, Herwig M, Sieme M, Delalat S, Mostafi N, Gömöri K, Tangos M, Jarkas M, Pabel S, Bruckmüller S, Skrygan M, Lódi M, Jaquet K, Sequeira V, Gambichler T, Remedios CD, Kovács Á, Mannherz HG, Mügge A, Sossalla S, Hamdani N. Stress activated signalling impaired protein quality control pathways in human hypertrophic cardiomyopathy. *Int J Cardiol*. 2021; **344**: 160–169.
  31. Lakatos BK, Ruppert M, Tokodi M, Oláh A, Braun S, Karime C, Ladányi Z, Sayour AA, Barta BA, Merkely B, Radovits T, Kovács A. Myocardial work index: A marker of left ventricular contractility in pressure- or volume overload-induced heart failure. *ESC Heart Fail*. 2021; **8**: 2220–2231.
  32. Guggilam A, Hutchinson KR, West TA, Kelly AP, Galantowicz ML, Davidoff AJ, Sadayappan S, Lucchesi PA. In vivo and in vitro cardiac responses to beta-adrenergic stimulation in volume-overload heart failure. *J Mol Cell Cardiol*. 2013; **57**: 47–58.
  33. Juric D, Yao X, Thandapilly S, Louis X, Cantor E, Chaze B, Wojciechowski P, Vasanthi Z, Yang T, Wigle J, Netticadan T. Defects in ryanodine receptor function are associated with systolic dysfunction in rats subjected to volume overload. *Exp Physiol*. 2010; **95**: 869–879.
  34. McGinley JC, Berretta RM, Chaudhary K, Rossman E, Bratinov GD, Gaughan JP, Houser S, Margulies KB. Impaired contractile reserve in severe mitral valve regurgitation with a preserved ejection fraction. *Eur J Heart Fail*. 2007; **9**: 857–864.
  35. Zheng J, Yancey DM, Ahmed MI, Wei CC, Powell PC, Shanmugam M, Gupta H, Lloyd SG, McGiffin DC, Schiros CG, Denney TS Jr, Babu GJ, Dell'Italia LJ. Increased sarcolipin expression and adrenergic drive in humans with preserved left ventricular ejection fraction and chronic isolated mitral regurgitation. *Circ Heart Fail*. 2014; **7**: 194–202.
  36. Adamcova M, Pelouch V. Isoforms of troponin in normal and diseased myocardium. *Physiol Res*. 1999; **48**: 235–247.
  37. Knott A, Purcell I, Marston S. In vitro motility analysis of thin filaments from failing and non-failing human heart: Troponin from failing human hearts induces slower filament sliding and higher ca(2+) sensitivity. *J Mol Cell Cardiol*. 2002; **34**: 469–482.
  38. Perry SV. Troponin I: Inhibitor or facilitator. *Mol Cell Biochem*. 1999; **190**: 9–32.
  39. van der Velden J, Papp Z, Zaremba R, Vandervelden J, Papp z, Zaremba R, Boontje N, Dejong J, Owen V, Burton P, Goldmann P, Jaquet K, Stienen G. Increased Ca2+–sensitivity of the contractile apparatus in end-stage human heart failure results from altered phosphorylation of contractile proteins. *Cardiovasc Res*. 2003; **57**: 37–47.
  40. Weber KT. Extracellular matrix remodeling in heart failure: A role for de novo angiotensin II generation. *Circulation*. 1997; **96**: 4065–4082.
  41. Heling A, Zimmermann R, Kostin S, Maeno Y, Hein S, Devaux B, Bauer E, Klövekorn WP, Schlepper M, Schaper W, Schaper J. Increased expression of cytoskeletal, linkage, and extracellular proteins in failing human myocardium. *Circ Res*. 2000; **86**: 846–853.
  42. Reil JC, Reil GH, Kovacs A, Kovács Á, Sequeira V, Waddingham MT, Lodi M, Herwig M, Ghaderi S, Kreusser MM, Papp Z, Voigt N, Dobrev D, Meyhöfer S, Langer HF, Maier LS, Linz D, Mügge A, Hohl M, Steendijk P, Hamdani N. CaMKII activity contributes to homeometric autoregulation of the heart: A novel mechanism for the Anrep effect. *J Physiol*. 2020; **598**: 3129–3153.
  43. Hamdani N, Kooij V, van Dijk S, Merkus D, Paulus WJ, Remedios C, Duncker DJ, Stienen GJM, van der Velden J. Sarcomeric dysfunction in heart failure. *Cardiovasc Res*. 2008; **77**: 649–658.
  44. Kooij V, Saes M, Jaquet K, Zaremba R, Foster DB, Murphy AM, dos Remedios C, van der Velden J, Stienen GJM. Effect of troponin I Ser23/24 phosphorylation on Ca2+–sensitivity in human myocardium depends on the phosphorylation background. *J Mol Cell Cardiol*. 2010; **48**: 954–963.
  45. Roman BB, Goldspink PH, Spaite E, Urbaniene D, McKinney R, Geenen DL, Solaro RJ, Buttrick PM. Inhibition of PKC phosphorylation of cTnI improves cardiac performance in vivo. *Am J Physiol Heart Circ Physiol*. 2004; **286**: H2089–H2095.
  46. Tong CW, Stelzer JE, Greaser ML, Powers PA, Moss RL. Acceleration of crossbridge kinetics by protein kinase a phosphorylation of cardiac myosin binding protein C modulates cardiac function. *Circ Res*. 2008; **103**: 974–982.
  47. Nagayama T, Takimoto E, Sadayappan S, Mudd JO, Seidman JG, Robbins J, Kass DA. Control of in vivo left ventricular [correction] contraction/relaxation kinetics by myosin binding protein C: Protein kinase a phosphorylation dependent and independent regulation. *Circulation*. 2007; **116**: 2399–2408.
  48. Kensler RW, Craig R, Moss RL. Phosphorylation of cardiac myosin binding protein C releases myosin heads from the surface of cardiac thick filaments.

- Proc Natl Acad Sci U S A.* 2017; **114**: E1355–E1364.
49. Ruppert M, Bodi B, Korkmaz-Icoz S, Bódi B, Korkmaz-Icöz S, Loganathan S, Jiang W, Lehmann L, Oláh A, Barta BA, Sayour AA, Merkely B, Karck M, Papp Z, Szabó G, Radovits T. Myofilament  $\text{Ca}^{2+}$  sensitivity correlates with left ventricular contractility during the progression of pressure overload-induced left ventricular myocardial hypertrophy in rats. *J Mol Cell Cardiol.* 2019; **129**: 208–218.
  50. Toischer K, Rokita AG, Unsöld B, Unsöld B, Zhu W, Kararigas G, Sossalla S, Reuter SP, Becker A, Teucher N, Seidler T, Grebe C, Preuß L, Gupta SN, Schmidt K, Lehnart SE, Krüger M, Linke WA, Backs J, Regitz-Zagrosek V, Schäfer K, Field LJ, Maier LS, Hasenfuss G. Differential cardiac remodeling in preload versus afterload. *Circulation.* 2010; **122**: 993–1003.
  51. Leite-Moreira AM, Almeida-Coelho J, Neves JS, Pires AL, Ferreira-Martins J, Castro-Ferreira R, Ladeiras-Lopes R, Conceição G, Miranda-Silva D, Rodrigues P, Hamdani N, Herwig M, Falcão-Pires I, Paulus WJ, Linke WA, Lourenço AP, Leite-Moreira AF. Stretch-induced compliance: A novel adaptive biological mechanism following acute cardiac load. *Cardiovasc Res.* 2018; **114**: 656–667.
  52. Labeit S, Kolmerer B. Titins: Giant proteins in charge of muscle ultrastructure and elasticity. *Science.* 1995; **270**: 293–296.
  53. Neagoe C, Kulke M, del Monte F, Gwathmey JK, de Tombe PP, Hajjar RJ, Linke WA. Titin isoform switch in ischemic human heart disease. *Circulation.* 2002; **106**: 1333–1341.
  54. Herwig M, Kolijn D, Lodi M, Lódi M, Hölper S, Kovács Á, Papp Z, Jaquet K, Haldenwang P, dos Remedios C, Reusch PH, Mügge A, Krüger M, Fielitz J, Linke WA, Hamdani N. Modulation of titin-based stiffness in hypertrophic cardiomyopathy via protein kinase D. *Front Physiol.* 2020; **11**: 240.
  55. Borbely A, Falcão-Pires I, van Heerebeek L, Borbely A, Hamdani N, Édes Í, Gavina C, Leite-Moreira AF, Bronzwaer JGF, Papp Z, van der Velden J, Stienen GJM, Paulus WJ. Hypophosphorylation of the stiff N2B titin isoform raises cardiomyocyte resting tension in failing human myocardium. *Circ Res.* 2009; **104**: 780–786.
  56. Hidalgo CG, Chung CS, Saripalli C, Methawasin M, Hutchinson KR, Tsapralis G, Labeit S, Mattiazzi A, Granzier HL. The multifunctional  $\text{Ca}^{2+}$ /calmodulin-dependent protein kinase II delta (CaMKII $\delta$ ) phosphorylates cardiac titin's spring elements. *J Mol Cell Cardiol.* 2013; **54**: 90–97.
  57. Erickson JR, Joiner ML, Guan X, Kutschke W, Yang J, Oddis CV, Bartlett RK, Lowe JS, O'Donnell SE, Aykin-Burns N, Zimmerman MC, Zimmerman K, Ham AJL, Weiss RM, Spitz DR, Shea MA, Colbran RJ, Mohler PJ, Anderson ME. A dynamic pathway for calcium-independent activation of CaMKII by methionine oxidation. *Cell.* 2008; **133**: 462–474.
  58. Fischer TH, Eiringhaus J, Dybkova N, Förster A, Herting J, Kleinwächter A, Ljubojevic S, Schmitto JD, Streckfuß-Bömeke K, Renner A, Gummert J, Hasenfuss G, Maier LS, Sossalla S.  $\text{Ca}^{2+}$ /calmodulin-dependent protein kinase II equally induces sarcoplasmic reticulum  $\text{Ca}^{2+}$  leak in human ischemic and dilated cardiomyopathy. *Eur J Heart Fail.* 2014; **16**: 1292–1300.
  59. Zhang T, Brown JH. Role of  $\text{Ca}^{2+}$ /calmodulin-dependent protein kinase II in cardiac hypertrophy and heart failure. *Cardiovasc Res.* 2004; **63**: 476–486.
  60. Purohit A, Rokita AG, Guan X, Chen B, Koval OM, Voigt N, Neef S, Sowa T, Gao Z, Luczak ED, Stefansdottir H, Behunin AC, Li N, el-Accaoui RN, Yang B, Swaminathan PD, Weiss RM, Wehrens XHT, Song LS, Dobrev D, Maier LS, Anderson ME. Oxidized  $\text{Ca}^{2+}$ /calmodulin-dependent protein kinase II triggers atrial fibrillation. *Circulation.* 2013; **128**: 1748–1757.
  61. Backs J, Song K, Bezprozvannaya S, Chang S, Olson EN. CaM kinase II selectively signals to histone deacetylase 4 during cardiomyocyte hypertrophy. *J Clin Invest.* 2006; **116**: 1853–1864.
  62. Passier R, Zeng H, Frey N, Naya FJ, Nicol RL, McKinsey TA, Overbeek P, Richardson JA, Grant SR, Olson EN. CaM kinase signaling induces cardiac hypertrophy and activates the MEF2 transcription factor in vivo. *J Clin Invest.* 2000; **105**: 1395–1406.
  63. Singh MV, Swaminathan PD, Luczak ED, Kutschke W, Weiss RM, Anderson ME. MyD88 mediated inflammatory signaling leads to CaMKII oxidation, cardiac hypertrophy and death after myocardial infarction. *J Mol Cell Cardiol.* 2012; **52**: 1135–1144.
  64. Luo M, Guan X, Luczak ED, Lang D, Kutschke W, Gao Z, Yang J, Glynn P, Sossalla S, Swaminathan PD, Weiss RM, Yang B, Rokita AG, Maier LS, Efimov IR, Hund TJ, Anderson ME. Diabetes increases mortality after myocardial infarction by oxidizing CaMKII. *J Clin Invest.* 2013; **123**: 1262–1274.
  65. Luczak ED, Anderson ME. CaMKII oxidative activation and the pathogenesis of cardiac disease. *J Mol Cell Cardiol.* 2014; **73**: 112–116.
  66. Burgoyne JR, Madhani M, Cuello F, Charles RL, Brennan JP, Schröder E, Browning DD, Eaton P. Cysteine redox sensor in PKGI $\alpha$  enables oxidant-induced activation. *Science.* 2007; **317**: 1393–1397.
  67. Prisyazhna O, Rudyk O, Eaton P. Single atom substitution in mouse protein kinase G eliminates oxidant sensing to cause hypertension. *Nat Med.* 2012; **18**: 286–290.
  68. Prisyazhna O, Burgoyne JR, Scotcher J, Grover S, Kass D, Eaton P. Phosphodiesterase 5 inhibition limits doxorubicin-induced heart failure by attenuating protein kinase G I $\alpha$  oxidation. *J Biol Chem.* 2016; **291**: 17427–17436.
  69. Nakamura T, Ranek MJ, Lee DI, Shalkey Hahn V, Kim C, Eaton P, Kass DA. Prevention of PKGI $\alpha$  oxidation augments cardioprotection in the stressed heart. *J Clin Invest.* 2015; **125**: 2468–2472.
  70. Oeing CU, Nakamura T, Pan S, Mishra S, Dunkerly-Eyring BL, Kokkonen-Simon KM, Lin BL, Chen A, Zhu G, Bedja D, Lee DI, Kass DA, Ranek MJ. PKGI $\alpha$  Cysteine-42 redox state controls mTORC1 activation in pathological cardiac hypertrophy. *Circ Res.* 2020; **127**: 522–533.
  71. Hamdani N, Hervent AS, Vandekerckhove L, Matheeußen V, Demolder M, Baerts L, de Meester I, Linke WA, Paulus WJ, de Keulenaer GW. Left ventricular diastolic dysfunction and myocardial stiffness in diabetic mice is attenuated by inhibition of dipeptidyl peptidase 4. *Cardiovasc Res.* 2014; **104**: 423–431.
  72. Bishu K, Hamdani N, Mohammed SF, Kruger M, Ohtani T, Ogut O, Brozovich FV, Burnett JC Jr, Linke WA, Redfield MM. Sildenafil and B-type natriuretic peptide acutely phosphorylate titin and improve diastolic distensibility in vivo. *Circulation.* 2011; **124**: 2882–2891.
  73. Hidalgo C, Hudson B, Bogomolovas J, Zhu Y, Anderson B, Greaser M, Labeit S, Granzier H. PKC phosphorylation of titin's PEVK element: A novel and conserved pathway for modulating myocardial stiffness. *Circ Res.* 2009; **105**: 631–638 617 p following 638.
  74. Zhang W, Elimban V, Nijjar MS, Gupta SK, Dhalla NS. Role of mitogen-activated protein kinase in cardiac hypertrophy and heart failure. *Exp Clin Cardiol.* 2003; **8**: 173–183.
  75. Fiedler B, Lohmann SM, Smolenski A, Linnemüller S, Pieske B, Schröder F, Molkentin JD, Drexler H, Wollert KC. Inhibition of calcineurin-NFAT hypertrophy signaling by cGMP-dependent protein kinase type I in cardiac myocytes. *Proc Natl Acad Sci U S A.* 2002; **99**: 11363–11368.
  76. Ahmed MI, Gladden JD, Litovsky SH, Lloyd SG, Gupta H, Inusah S, Denney T Jr, Powell P, McGiffin DC, Dell'Italia LJ. Increased oxidative stress and cardiomyocyte myofibrillar degeneration in patients with chronic isolated mitral regurgitation and ejection fraction >60%. *J Am Coll Cardiol.* 2010; **55**: 671–679.

77. Chen YW, Pat B, Gladden JD, Zheng J, Powell P, Wei CC, Cui X, Husain A, Dell'Italia LJ. Dynamic molecular and histopathological changes in the extracellular matrix and inflammation in the transition to heart failure in isolated volume overload. *Am J Physiol Heart Circ Physiol.* 2011; **300**: H2251–H2260.
78. Corcoran A, Cotter TG. Redox regulation of protein kinases. *FEBS J.* 2013; **280**: 1944–1965.